Materials Letters 67 (2012) 74–77

Contents lists available at SciVerse ScienceDirect

Materials Letters

journal homepage: www.elsevier.com/locate/matlet

# Synthesis of symmetrical hexagonal-shape PbO nanosheets using gold nanoparticles

Shuwen Zeng [a,b,c], Yennan Liang [d], Haifei Lu [c,e], Libo Wang [d], Xuan-Quyen Dinh [b], Xia Yu [c], Ho-Pui Ho [e], Xiao Hu [d], Ken-Tye Yong [a,*]

[a] School of Electrical and Electronic Engineering, Nanyang Technological University, Singapore 639798, Singapore
[b] CINTRA CNRS/NTU/THALES, UMI 3288, Research Techno Plaza, 50 Nanyang Drive, Border X Block, Singapore, 637553
[c] Singapore Institute of Manufacturing Technology, 71 Nanyang Drive, Singapore, 638075
[d] School of Materials Science and Engineering, Nanyang Technological University, Singapore 639798, Singapore
[e] Department of Electronic Engineering, The Chinese University of Hong Kong, Hong Kong Peoples R China

ARTICLE INFO

*Article history:*
Received 11 July 2011
Accepted 8 September 2011
Available online 17 September 2011

*Keywords:*
Nanocrystals
Gold nanoparticles
Nanosheet
Anisotropic growth
Lead oxide

ABSTRACT

Anisotropic growth of PbO with symmetrical hexagonal-shape nanosheet morphology was demonstrated for the first time via solution phase synthesis in the presence of Au nanoparticles at room temperature. Au NPs play a critical role in the formation of PbO nanosheets. No nanosheets were formed in absence of Au NPs. The effect of Au NPs appears to result from their ability to provide nucleation sites to seed anisotropic growth of the PbO nanocrystals and later the nanocrystals aggregated to form nanosheet structure. The method demonstrated here provides a facile room temperature colloidal method of producing high-quality and yield of high-symmetrical hexagonal-shape PbO nanosheets with controlled edge length.



## 1. Introduction

Functionalized nanomaterials have received intense research interests due to their potential applications ranging from biosensors and drug delivery to the design of nanoformulations for therapy [1–3]. Among them, gold nanoparticles (Au NPs) are considered to be an excellent candidate for the applications mentioned above due to their unique electronic and optical properties [4–7]. For example, Au NPs display unique optical properties including a strong surface plasmon resonance (SPR) with high quantum efficiency and resistance to photobleaching, whereby making them visible by laser scanning confocal microscopy and detectable at a single particle level. Also, the SPR peak can be tuned from 520 to 1200 nm by manipulating the Au NPs size, aspect ratio, and interparticle spacing [8, 9].

Recently, there is a growing interest in terms of shape and structure control of nanocrystals by seeding their growth with Au NPs under different reaction temperature [10–17]. For example, Yong et al. [12, 14] demonstrated that CdSe, CdS, PbS, and PbSe nanocrystals with different morphologies such as wires, plates, multipods, cubes, crosses, stars, and branched structures were synthesized in the presence of Au NPs at 150 °C. It was discovered that the important parameter in dictating the shape, size and structure of nanocrystals is the concentration of the metal NPs and the precursor ratio. Shi et al [15] demonstrated a strategy for preparing binary and ternary hybrid nanoparticles based on spontaneous epitaxial nucleation and growth of a second and third component onto Au NPs at temperature as high as 300 °C. All these examples have pinpointed that Au NPs can be served as a nucleation site for seeding the growth of various shape and structure of nanocrystals using appropriate reaction conditions.

Here, we demonstrate for the first time the fabrication of hexagonal PbO nanosheet using Au NPs as seeds at room temperature which is in contrast with present methods involving high temperature and complex steps. The formation of the PbO nanosheet strongly depends on the presence of the Au NPs, and on the Pb concentration in the growth solution. The present approach does not use any organic surfactants that are frequently used for controlling the shape and structure of nanocrystals such as oleic acid and trioctylphosphine oxide (TOPO). More importantly, the reaction temperature and reagent concentrations used here are much lower than those previously reported for PbO nanocrystals synthesis. The Au NPs facilitate nucleation and growth of PbO nanosheet at these relatively mild conditions since no high reaction temperature and toxic surfactants are used.

## 2. Materials and methods

### 2.1. Preparation of Au nanoparticles

The synthesis of gold colloids typically involves the reduction of gold salts in the presence of surfactants or stabilizers [18]. In brief, 10 ml of $HAuCl_4$ (5 mM) solution was added to a flask containing 85 ml of boiling distilled water, and the mixture was allowed to return to a boil. Then, a freshly prepared sodium citrate solution

* Corresponding author. Tel.: +65 6790 5444; fax: +65 6793 3318.
*E-mail address:* ktyong@ntu.edu.sg (K.-T. Yong).

0167-577X/$ – see front matter © 2011 Elsevier B.V. All rights reserved.
doi:10.1016/j.matlet.2011.09.048

(5 ml, 0.03 M) was added to the mixture. A few minutes later, the solution changed from colorless to a deep wine-red. The resulting red sol contained citrate-gold nanoparticles of approximately 12 nm in diameter.

### 2.2. Synthesis of lead oxide nanosheet

Lead acetate solution was prepared at different concentrations ranging from 0.01 to 4 mM. Next, lead acetate solution (10 mL) with different concentrations was mixed with fixed volume concentration of Au NPs. After gentle stirring, the solution with lead acetate concentrations above 0.2 mM was observed to change from red to blue. The solutions were then left undisturbed at room temperature for 24 h. After 24 h, hexagonal PbO nanosheets were formed in the solutions at lead acetate concentration above 0.9 mM.

### 2.3. Characterization methods

High resolution transmission electron microscopy (HRTEM) images were obtained using a JEOL model JEM 2010 microscope at an acceleration voltage of 200 kV. The specimens were prepared by drop-coating the sample dispersion onto a carbon-coated copper grid, which was placed on filter paper to absorb excess solvent. Scanning electron microscopy (SEM) images were obtained using Zeiss EVO50 extended pressure microscope at an acceleration voltage of 20 kV. X-ray powder diffraction patterns were recorded using a Bruker D8 Discover X-ray diffractometer with Cu Kα radiation. Atomic force microscopy (AFM) images were obtained from NanoScope Dimension 3000. Absorption spectra of nanoparticle solutions were collected with Shimadzu UV-3101 UV–vis–near-IR spectrophotometer.

## 3. Results and discussion

Hexagonal PbO nanosheets were synthesized, as described above, upon introducing lead acetate solution into reaction mixture containing 12 nm diameter Au NPs. The formation of the PbO nanosheet strongly depended on the concentration of the Au NPs and on the lead acetate concentration in the growth solution. Using lead acetate concentration of 0.9 mM and with the presence of Au NPs, hexagonal PbO nanosheets were obtained as a mixture of majority of individual nanocrystal and minor irregular shape nanocrystals. Uniform thickness nanosheets were produced upon aging the mixture for more than 20 h. Fig. 1a shows SEM images of nanosheets with a size ranging from 2 to 2.5 μm. The TEM images, and selected area electron diffraction (SAED) pattern from the HRTEM demonstrate the high degree of crystallinity and narrow diameter distribution of the nanosheets. Fig. 1c shows AFM image of nanosheet with a uniform thickness of 110 nm. The compositions of the prepared nanosheets were further confirmed by the EDS and it is evident that the nanosheet samples are mainly composed of lead and oxygen (see Fig. 1d). No formation of the nanosheets was observed in the absent of the Au NPs.

The structure of the PbO nanosheets was further examined by powder X-ray diffraction (XRD). The diffractogram shown in Fig. 2 is consistent with the bulk rock salt structure of PbO. The three strong peaks with 2θ values of 27.18°, 34.05°, 49.26° and 58.09° correspond to the (111), (200), (220) and (311) planes, respectively. The Au NPs concentration is too low to show any characteristic XRD peaks, which would appear at 2θ values of 38.18°, 44.39° and 64.57°. Fig. 1(b) show HRTEM image of the PbO nanosheet. This image indicates that the nanosheet is crystalline and exhibit well-resolved lattice fringes.

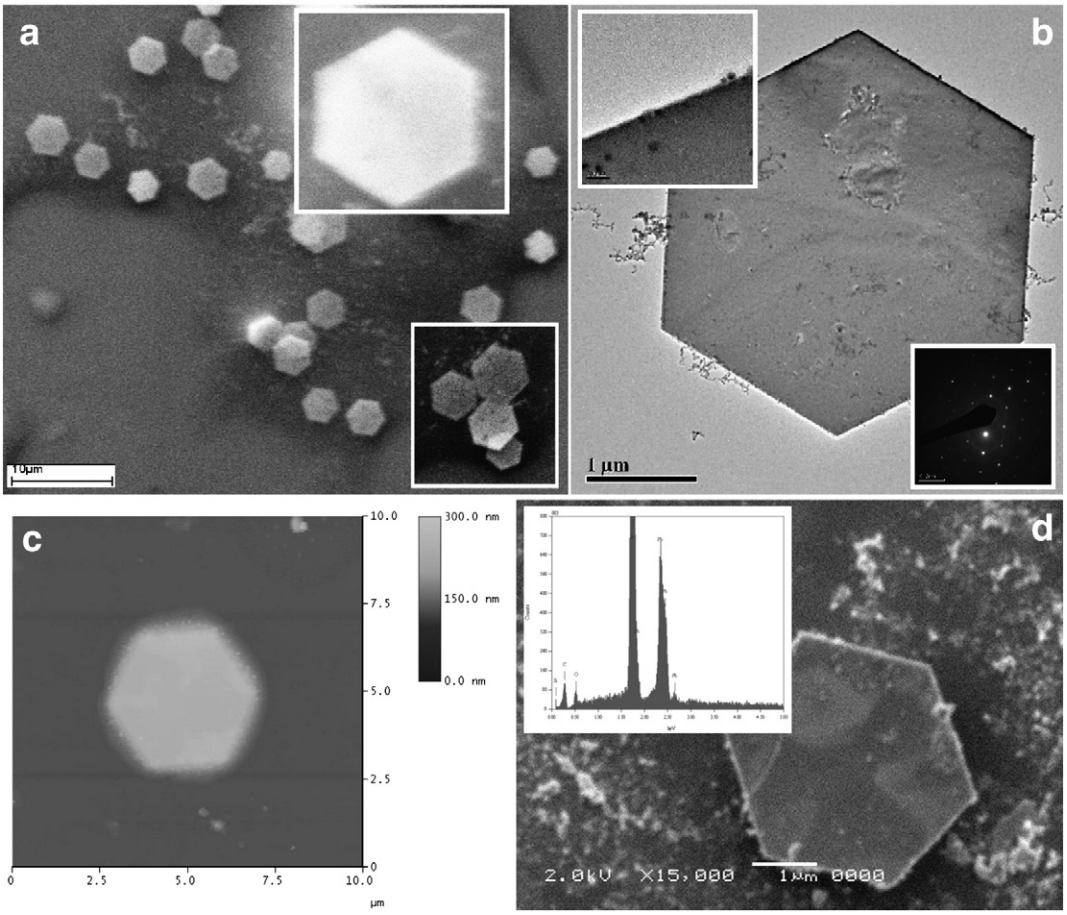


**Fig. 1.** (a) SEM image of a large quantity of hexagonal-shape PbO nanosheets. (b) TEM image of PbO nanosheets showing that they are highly symmetry in their edge length. The average size of the nanosheet is 2.5 μm. The edge length of the nanosheet is above 1.5 μm. (c) AFM image of a PbO nanosheet, showing thickness of 110 nm. (d) EDS elemental analysis of the PbO nanosheet.

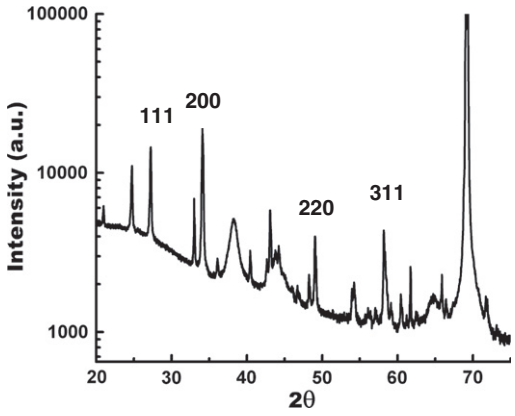


**Fig. 2.** XRD pattern of PbO nanosheets as those shown in Fig. 1.

To study the formation process of the hexagonal PbO nanosheet in the presence of Au NPs, reaction solution was removed from the reaction mixture at different time points. The reaction solution was then removed from the growth solution and characterized using TEM. Fig. 3 shows the progression of the formation of PbO nanosheets from aggregation of PbO nanoparticles. Initially, PbO nanoparticles were formed on the Au NPs surface as shown in Fig. 3a. Fig. 3e shows the HRTEM image of Au NPs seeding the growth of PbO nanoparticles. Subsequently, further aging the reaction mixture, the PbO nanoparticles were observed to fuse together and result the "premature stage" of hexagonal shape PbO nanosheets as shown in Fig. 3b and c. The edges of these "premature stage" PbO nanosheets were corrugated as shown in Fig. 3d. Upon aging these particles with 24 h, large PbO nanosheets were formed as those shown in Fig. 1. It is worth noting that larger nanosheets can be produced upon increasing the concentration of lead acetate in the growth solution.

Tang et al. [19] reported that CdTe nanosheets were synthesized by precipitating and aging CdTe nanoparticles in deionized water. They proposed that anisotropic electrostatic interactions arising from both a dipole moment and a small positive charge, combined with directional hydrophobic attraction, are responsible for the formation of the free-floating nanosheets. The authors have used molecular simulations based on a coarse-grained model with proper parameters determined by semi-empirical quantum mechanics calculations were performed to prove the hypothesis. Schliehe et al. [20] reported the fabrication of ultrathin single-crystal PbS sheets with dimensions on the micrometer scale using hot colloidal synthesis method. The PbS ultrathin sheets are formed in the presence of chlorine containing compounds such as 1,2-dichloroethane or similar linear chloroalkanes. The nanosheets have lateral dimensions of several hundred nanometers. The authors have suggested that the formation of PbS ultrathin sheets is originated from the oriented attachment of the PbS nanoparticles in a two-dimensional fashion. Here, PbO nanosheet formation is more likely to result from an oriented attachment mechanism, in which the sheets form by aggregation of small nanoparticle that each has a net dipole moment [21]. This has been observed in other semiconductors. The process is driven by the reduction in surface area that happens during aggregation. In the formation of PbS nanosheet demonstrated by Schliehe et al., they explained this result by a faster growth rate perpendicular to the [111] facets. Their findings also suggest that [110] facets are highly reactive and, therefore, are preferentially consumed during the nanoparticle growth. Basically, during the sheet-like crystal growth, the particles try to minimize the most energetically unfavorable surface facets by fast growth perpendicular to the respective facet. We speculate that this process may be responsible for the two-dimensional growth of the PbO nanocrystals. Also, we suggest that Oswald ripening process [22] may contribute some effects towards the formation of the sheet under long reaction period of time.

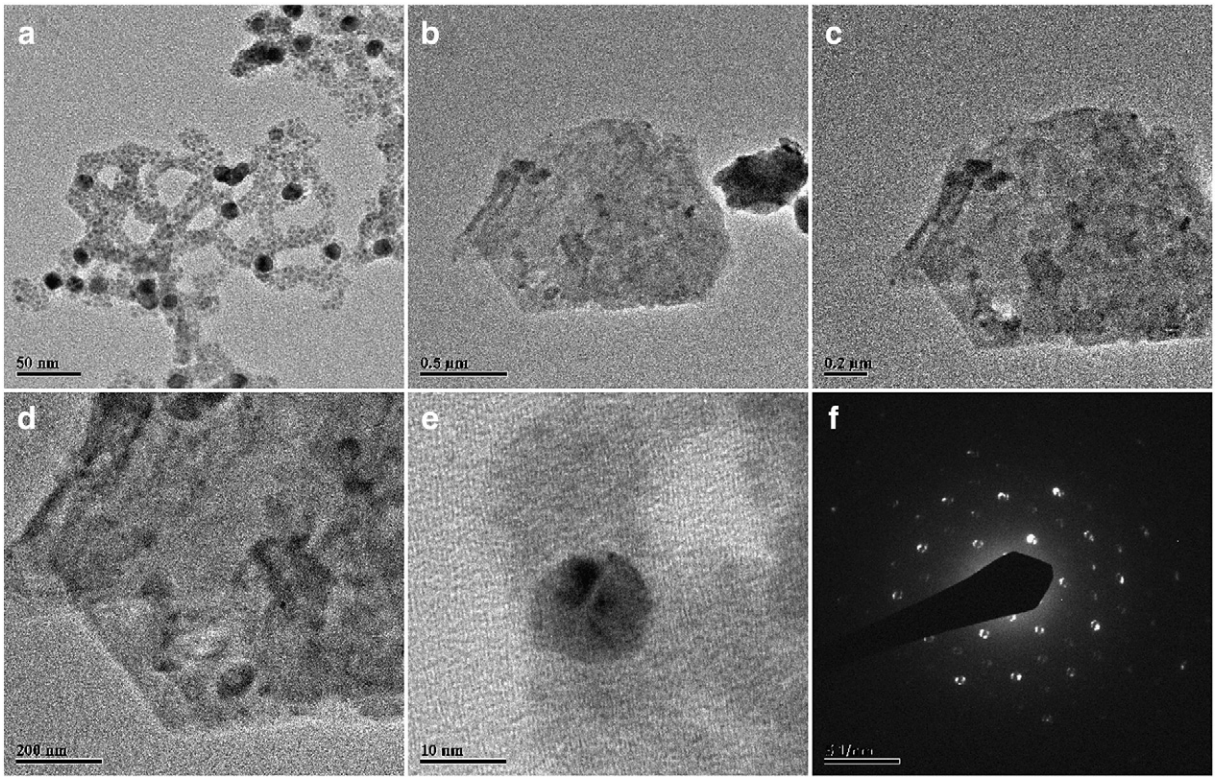


**Fig. 3.** Growth of PbO nanosheets in the presence of Au NPs. (a) Formation of PbO nanocrystals on the Au NPs surface. (b) Early stage of PbO nanosheets formation. (c and d) High resolution TEM image of PbO nanosheets. (e) PbO nanocrystal forming on the surface of Au NPs. (f) Selected area electron diffraction (SAED) pattern for PbO nanosheet in Fig. 3d.

## 4. Conclusions

The synthesis of hexagonal-shape, high symmetrical crystalline PbO nanosheets were achieved using Au NPs as seeds at room temperature. No PbO nanosheets were formed in the absence of Au NPs suggesting that Au NPs can serve as a nucleation site to promote the growth of PbO nanosheets. High quality of the PbO nanosheets were obtained in the presence of Au NPs, apparently due to the ability of the Au seed particles to provide sites for heterogeneous nucleation and anisotropic growth of PbO nanosheets. In the near future, we envision that the developed method could be used for synthesizing metal-oxide based anisotropic nanocrystals in the presence of Au NPs.

## Acknowledgements

The authors would like to thank Dr. Sim Lay May from Singapore Institute of Manufacturing Technology for assistance in XRD measurement. This work is partially supported by Joint Council Office grant (10/3/EG/05/01).

## References

[1] Schmid G, editor. Clusters and Colloids - From Theory to Applications. Weinheim, Germany: VCH; 1994.
[2] Burda C, et al. Chemistry and properties of nanocrystals of different shapes. Chem Rev 2005;105(4):1025–102.
[3] Alivisatos P. The use of nanocrystals in biological detection. Nat Biotechnol 2004;22(1):47–52.
[4] Daniel MC, Astruc D. Gold nanoparticles: assembly, supramolecular chemistry, quantum-size-related properties, and applications toward biology, catalysis, and nanotechnology. Chem Rev 2004;104(1):293–346.
[5] Wilson R. The use of gold nanoparticles in diagnostics and detection. Chem Soc Rev 2008;37(9):2028–45.
[6] Ghosh P, et al. Gold nanoparticles in delivery applications. Adv Drug Deliv Rev 2008;60(11):1307–15.
[7] Zeng S, et al. A review on functionalized gold nanoparticles for biosensing applications. Plasmonics 2011;6(3):491–506.
[8] Njoki PN, et al. Size correlation of optical and spectroscopic properties for gold nanoparticles. J Phys Chem C 2007;111(40):14664–9.
[9] Link S, El-Sayed MA. Size and temperature dependence of the plasmon absorption of colloidal gold nanoparticles. J Phys Chem B 1999;103(21):4212–7.
[10] Ah CS, Do Hong S, Jang DJ. Preparation of AucoreAgshell nanorods and characterization of their surface plasmon resonances. J Phys Chem B 2001;105(33):7871–3.
[11] Lee JS, Shevchenko EV, Talapin DV. Au–PbS core–shell nanocrystals: plasmonic absorption enhancement and electrical doping via intra-particle charge transfer. J Am Chem Soc 2008;130(30):9673–5.
[12] Yong KT, et al. Shape control of PbSe nanocrystals using noble metal seed particles. Nano Lett 2006;6(4):709–14.
[13] Yong KT, et al. Control of the morphology and size of PbS nanowires using gold nanoparticles. Chem Mater 2006;18(25):5965–72.
[14] Yong KT, et al. Shape control of CdS nanocrystals in one-pot synthesis. J Phys Chem C 2007;111(6):2447–58.
[15] Shi WL, et al. A general approach to binary and ternary hybrid nanocrystals. Nano Lett 2006;6(4):875–81.
[16] Lee I, et al. Nanoparticle directed crystallization of calcium carbonate. Adv Mater 2001;13(21):1617–20.
[17] Jana NR, Gearheart L, Murphy CJ. Evidence for seed-mediated nucleation in the chemical reduction of gold salts to gold nanoparticles. Chem Mater 2001;13(7):2313–22.
[18] Frens G. Controlled nucleation for regulation of particle-size in monodisperse gold suspensions. Nat Phys Sci 1973;241(105):20–2.
[19] Tang ZY, et al. Self-assembly of CdTe nanocrystals into free-floating sheets. Science 2006;314(5797):274–8.
[20] Schliehe C, et al. Ultrathin PbS sheets by two-dimensional oriented attachment. Science 2010;329(5991):550–3.
[21] Talapin DV, et al. Dipole-dipole interactions in nanoparticle superlattices. Nano Lett 2007;7(5):1213–9.
[22] Yang WY, et al. Ostwald ripening growth of silicon nitride nanoplates. Cryst Growth Des 2010;10(1):29–31.